On the Performance of a Persymmetric Adaptive Matched Filter

JUN LIU, Member, IEEE
Xidian University
Xi'an, China

GUOLONG CUI, Member, IEEE
University of Electronic Science and Technology of China
Chengdu, China

HONGBIN LI, Senior Member, IEEE
Stevens Institute of Technology
Hoboken, NJ, USA

BRAHAM HIMED, Fellow, IEEE
AFRL/RYMD
Dayton, OH, USA

We examine the adaptive detection problem in the presence of colored noise with an unknown covariance matrix, by exploiting a persymmetric structure in the received signal. The persymmetric adaptive matched filter (PS-AMF) is used to address this problem, which can significantly alleviate the requirement of secondary data. In G. Pailloux et al. "Persymmetric adaptive radar detectors," (2011) the probability of false alarm of the PS-AMF has been obtained in terms of the Gaussian hypergeometric function. In this paper, finite-sum expressions for the probability of false alarm of the PS-AMF are derived, which are more convenient to use in calculating the detection threshold. Moreover, the detection probabilities of the PS-AMF for both nonfluctuating and fluctuating target models are derived. In the fluctuating model, the amplitude of the target echoes is described by a generalized Chi distribution that involves the Rayleigh distribution as a special case. These theoretical results are all confirmed using Monte Carlo (MC) simulations.

Manuscript received August 26, 2014; revised January 15, 2015, March 17, 2015; released for publication March 20, 2015.

DOI. No. 10.1109/TAES.2015.140633.

Refereeing of this contribution was handled by F. Gini.

Authors' current addresses: J. Liu, National Laboratory of Radar Signal Processing, Xidian University, Xi'an, 710071, China; G. Cui, School of Electronic Engineering, University of Electronic Science and Technology of China, Chengdu, China; H. Li, Stevens Institute of Technology, Department of Electrical and Computer, Engineering, Castle Point on Hudson, Hoboken, NJ 07030. E-mail: (hongbin.li@stevens.edu). B. Himed, Air Force Research Laboratory, Sensors Directorate, 2241 Avionics Circle, WPAFB, OH 45433.

I. INTRODUCTION

The problem of adaptive detection in colored noise with an unknown covariance matrix is commonly encountered in many applications such as radar, sonar, and communications. To deal with this problem, a standard approach is to employ a set of secondary data (training data) to estimate the covariance matrix. This has led to the development of several seminal detectors, e.g., Kelly's generalized likelihood ratio test (GLRT) [2], adaptive matched filter (AMF) [3], and adaptive subspace detector [4]. Numerous studies of these detectors have been reported in the literature, including performance analysis [5–7], extensions for applications in multi-input multi-output (MIMO) radar [8–10], and polarimetric radar [11, 12], among others. Interestingly, all these detectors ensure constant false alarm rate (CFAR) properties with respect to the noise covariance matrix. It is well known that the loss in detection performance of the adaptive detectors with respect to the nonadaptive matched filter (MF) is 3 dB when the amount of training data used to estimate the noise covariance matrix is approximately twice the dimension of the received signal [13]. The requirement on the number of the training data may be restrictive. In many practical scenarios, it is difficult to collect sufficient target-free training data to meet the training requirement, due to many factors such as variations in terrain and interfering targets [14]. Therefore, it is of importance to investigate how to achieve satisfactory detection performance when the amount of training data is limited.

Note that all the detectors mentioned above do not exploit any structural information on the noise covariance matrix. In practical applications, the noise covariance matrix has a Hermitian persymmetric (also called centrohermitian) form, when the used system is equipped with a symmetrically spaced linear array for spatial processing or symmetrically spaced pulse trains for temporal processing [15]. Hermitian persymmetry has a property of double symmetry, i.e., Hermitian about its principal diagonal and persymmetric about its cross diagonal. Unless otherwise stated, "persymmetric" always denotes "Hermitian persymmetric" for brevity in the following. Note that the persymmetry includes as a special case the Toeplitz structure existing in a uniformly spaced array or pulse train. The persymmetric structure information has been applied in many scenarios, such as direction-of-arrival estimation [16], detection [1, 17], and adaptive beamforming [18].

The investigation on the persymmetric structure of the noise covariance matrix can be traced to Nitzberg's paper [19], where the maximum likelihood (ML) estimate of the persymmetric covariance matrix is obtained. Using this ML estimate, Cai and Wang developed two persymmetric detection algorithms, i.e., the persymmetric multiband GLRT algorithm [15] and the persymmetric sample matrix inversion (SMI) algorithm [20]. In recent years, many other detection algorithms have been proposed with a

priori information on the persymmetric structure of the noise covariance matrix [1, 17, 21–25]. All these persymmetric detection algorithms mentioned above validate the fact that a notable gain in detection performance can be obtained by exploiting the persymmetric structure in the noise covariance, especially when the amount of training data available is limited.

In [1], a persymmetric adaptive matched filter (PS-AMF) is proposed, which is an extension of the AMF in [3] from the unstructured case to the persymmetric case. The authors in [1] have derived an expression for the probability of false alarm of the PS-AMF in terms of the Gaussian hypergeometric function that involves integration and may not be convenient to use for the calculation of the detection threshold given a probability of false alarm. In addition, the detection probability of the PS-AMF is not provided in [1]. Therefore, a more comprehensive investigation on the performance of the PS-AMF is needed. In principle, the theoretical analysis of the PS-AMF can be conducted by using an approach similar to that in [26]. As shown in [26], nevertheless, the derivation is lengthy and complicated.

In this paper, the statistical properties of the PS-AMF are obtained in a simple method which is different from that in [26]. More specifically, we derive elementary expressions for the probability of false alarm of the PS-AMF in two special cases where the amount of secondary data is about half of the dimension of the received signal. In other cases, the probability of false alarm can be well approximated by an elementary expression due to the Laplace approximation of the Gaussian hypergeometric function. These elementary expressions for the probability of false alarm are easier to use in setting the test threshold than the Gaussian hypergeometric function in [1]. Furthermore, closed-form expressions for the detection probability of the PS-AMF are derived for both nonfluctuating and fluctuating target models. In the nonfluctuating model, the target echoes are deterministic, whereas in the fluctuating model, the amplitude of the target echoes is assumed to have a generalized Chi distribution and the phase of the target echoes is uniformly distributed in $[0, 2\pi)$ [27]. These theoretical results are all verified by using Monte Carlo (MC) simulations. Finally, numerical simulations are provided to demonstrate the performance of the PS-AMF.

The remainder of this paper is organized as follows. Section II formulates the problem to be studied. In Section III, a detailed performance analysis of the PS-AMF is provided. Simulation results are illustrated in Section IV and finally the paper is summarized in Section V.

Notation: Vectors (matrices) are denoted by boldface lower (upper) case letters. Superscripts $(\cdot)^T$, $(\cdot)^*$, and $(\cdot)^\dagger$ denote transpose, complex conjugate, and complex conjugate transpose, respectively. The notation $\sim$ means "is distributed as," and $\mathcal{CN}$ denotes a circularly symmetric, complex Gaussian distribution. $\mathbf{I}_p$ stands for a p-dimensional identity matrix. For any matrix $\mathbf{B}$, the (i, j)-th entry is denoted by $b_{i,j}$. $|\cdot|$ represents the modulus of a complex number and $\jmath = \sqrt{-1}$. $\det(\cdot)$ and $\mathrm{tr}(\cdot)$ denote the determinant and trace of a matrix, respectively. $\Gamma(\cdot)$ is the Gamma function. $\Re\mathfrak{e}$ and $\Im\mathfrak{m}$ represent the real and imaginary parts of a complex quantity, respectively. $\stackrel{\mathrm{d}}{=}$ means the random quantities on both sides of the equation have the same distribution. $\mathcal{W}_n(K, \mathbf{R})$ is an n-dimensional complex Wishart distribution with K degrees of freedom (DOFs) and parameter matrix $\mathbf{R}$. C_n^m is the binomial coefficient. χ_n^2 denotes the central Chi-squared distribution with n DOFs, and $\chi_n'^2(v)$ is the noncentral Chi-squared distribution with n DOFs and noncentrality parameter v.

II. PROBLEM FORMULATION

Consider the following hypothesis testing problem:

$$H_0 : \begin{cases} \mathbf{y} = \mathbf{c} \sim \mathcal{CN}(\mathbf{0}, \mathbf{M}) \\ \mathbf{y}_k = \mathbf{c}_k \sim \mathcal{CN}(\mathbf{0}, \mathbf{M}), \quad k = 1, \ldots, K, \end{cases} \tag{1a}$$

and

$$H_1 : \begin{cases} \mathbf{y} = a\mathbf{p} + \mathbf{c} \sim \mathcal{CN}(a\mathbf{p}, \mathbf{M}) \\ \mathbf{y}_k = \mathbf{c}_k \sim \mathcal{CN}(\mathbf{0}, \mathbf{M}), \quad k = 1, \ldots, K, \end{cases} \tag{1b}$$

where $\mathbf{p}$ is a known steering vector of dimension $m \times 1$; a is a deterministic but unknown complex scalar accounting for the target reflectivity and the channel propagation effects; the noise $\mathbf{c}$ is assumed to have circularly symmetric, complex Gaussian distribution, i.e., $\mathbf{c} \sim \mathcal{CN}(\mathbf{0}, \mathbf{M})$, where $\mathbf{M}$ is a positive definite covariance matrix of dimension $m \times m$.

When the system is equipped with a symmetrically spaced linear array for spatial domain processing or symmetrically spaced pulse trains for temporal domain processing, $\mathbf{p}$ and $\mathbf{M}$ possess persymmetric structures. More specifically,

$$\mathbf{M} = \mathbf{J}\mathbf{M}^*\mathbf{J} \quad \text{and} \quad \mathbf{p} = \mathbf{J}\mathbf{p}^*, \tag{2}$$

where $\mathbf{J}$ is a permutation matrix given as

$$\begin{bmatrix} 0 & 0 & \cdots & 0 & 1 \\ 0 & 0 & \cdots & 1 & 0 \\ \vdots & \vdots & \vdots & \vdots & \vdots \\ 0 & 1 & \cdots & 0 & 0 \\ 1 & 0 & \cdots & 0 & 0 \end{bmatrix}. \tag{3}$$

Based on the persymmetric structure in the received data, we can use a unitary matrix to transform the complex quantities $\mathbf{p}$ and $\mathbf{M}$ to real ones. Such a unitary matrix is given by [1]

$$\mathbf{T} = \begin{cases} \frac{1}{\sqrt{2}} \begin{pmatrix} \mathbf{I}_{m/2} & \mathbf{J}_{m/2} \\ \jmath\mathbf{I}_{m/2} & -\jmath\mathbf{J}_{m/2} \end{pmatrix} & \text{for } m \text{ is even,} \\ \frac{1}{\sqrt{2}} \begin{pmatrix} \mathbf{I}_{(m-1)/2} & 0 & \mathbf{J}_{(m-1)/2} \\ 0 & \sqrt{2} & 0 \\ \jmath\mathbf{I}_{(m-1)/2} & 0 & -\jmath\mathbf{J}_{(m-1)/2} \end{pmatrix} & \text{for } m \text{ is odd.} \end{cases} \tag{4}$$

Applying this unitary transform to the received data results in

$$H_0 : \begin{cases} \mathbf{x} = \mathbf{n} \sim \mathcal{CN}(\mathbf{0}, \mathbf{R}) \\ \mathbf{x}_k = \mathbf{n}_k \sim \mathcal{CN}(\mathbf{0}, \mathbf{R}) \end{cases} \tag{5a}$$

and

$$H_1 : \begin{cases} \mathbf{x} = a\mathbf{s} + \mathbf{n} \sim \mathcal{CN}(a\mathbf{s}, \mathbf{R}) \\ \mathbf{x}_k = \mathbf{n}_k \sim \mathcal{CN}(\mathbf{0}, \mathbf{R}) \end{cases}, \tag{5b}$$

where

$$\mathbf{x} = \mathbf{T}\mathbf{y} \in \mathbb{C}^m, \tag{6}$$

$$\mathbf{x}_k = \mathbf{T}\mathbf{y}_k \in \mathbb{C}^m, \tag{7}$$

$$\mathbf{s} = \mathbf{T}\mathbf{p} \in \mathbb{R}^m, \tag{8}$$

$$\mathbf{n} = \mathbf{T}\mathbf{c} \sim \mathcal{CN}(\mathbf{0}, \mathbf{R}) \tag{9}$$

with

$$\mathbf{R} = \mathbf{T}\mathbf{M}\mathbf{T}^\dagger \in \mathbb{R}^{m\times m}. \tag{10}$$

It is worth noting that $\mathbf{s}$ and $\mathbf{R}$ are both real. As shown in [1], the ML estimator $\hat{\mathbf{R}}$ of the real covariance matric $\mathbf{R}$ is

$$\hat{\mathbf{R}} = \mathfrak{Re}\left(\frac{1}{K}\sum_{k=1}^{K}\mathbf{x}_k\mathbf{x}_k^\dagger\right). \tag{11}$$

Moreover,

$$2K\hat{\mathbf{R}} \sim \mathcal{W}_m(2K, \mathbf{R}). \tag{12}$$

Therefore, the AMF using the persymmetric structures becomes

$$\Lambda_{\text{PS-AMF}} = \frac{|\mathbf{s}^T\hat{\mathbf{R}}^{-1}\mathbf{x}|^2}{\mathbf{s}^T\hat{\mathbf{R}}^{-1}\mathbf{s}} \underset{H_0}{\overset{H_1}{\gtrless}} \lambda, \tag{13}$$

where λ is the detection threshold. This detector is referred to as the PS-AMF. In the sequel, we provide a statistical analysis of this detector, and derive closed-form expressions for the probabilities of false alarm and detection.

III. PERFORMANCE ANALYSIS

A. Probability of False Alarm

The probability of false alarm of the PS-AMF has been derived in [1, eq. (55)] in terms of the Gaussian hypergeometric function, i.e.,

$$P_{\text{FA}} = {}_2F_1\left(M, M+\frac{1}{2}; K+\frac{1}{2}; -\frac{\lambda}{K}\right), \tag{14}$$

where

$$M = \frac{2K-m+1}{2}, \tag{15}$$

and ${}_2F_1(\cdot)$ denotes the hypergeometric function given by

$${}_2F_1(n_1, n_2;\ n_3;\ \tilde{x}) = \frac{\Gamma(n_3)}{\Gamma(n_2)\Gamma(n_3-n_2)} \times \int_0^1 \frac{t^{n_2-1}(1-t)^{n_3-n_2-1}}{(1-t\tilde{x})^{n_1}}\mathrm{d}t. \tag{16}$$

It is not convenient to set the detection threshold by using (14), since the Gaussian hypergeometric function is in an integral form. In the following, we develop a simpler method to calculate the detection threshold.

In the extreme cases where the number of secondary samples is about half the dimension of the primary data vector, the expression for the probability of false alarm can be written in terms of elementary functions. Such two cases are listed below.

Case 1: when m is even and $K = m/2$, we have $M = 1/2$. Then, the probability of false alarm in (14) can be cast as

$$\begin{aligned} P_{\text{FA}} &= {}_2F_1\left(\frac{1}{2}, 1;\ K+\frac{1}{2}; -\frac{\lambda}{K}\right) \\ &= {}_2F_1\left(1, \frac{1}{2};\ K+\frac{1}{2}; -\frac{\lambda}{K}\right) \\ &= \left[2\sqrt{z}\tanh^{-1}(\sqrt{z}) + \sum_{k=1}^{K-2}\frac{(k-1)!}{\left(\frac{1}{2}\right)_K}\left(\frac{z}{z-1}\right)^k\right] \\ &\quad \times \frac{\left(\frac{1}{2}\right)_K(z-1)^{K-1}}{(K-1)!z^K}, \end{aligned} \tag{17}$$

where $z = -\frac{\lambda}{K}$, the third equality is obtained by using [28, p. 463, eq. 7.3.1.137], the Pochhammer symbol $(a)_n$ and the inverse hyperbolic tangent function $\tanh^{-1}(x)$ are defined as

$$(a)_n = \frac{\Gamma(a+n)}{\Gamma(a)}, \tag{18}$$

and

$$\tanh^{-1}(x) = \frac{1}{2}[\ln(1+x) - \ln(1-x)], \tag{19}$$

respectively.

Case 2: when m is odd and $K = \frac{m+1}{2}$, we have $M = 1$. Then,

$$\begin{aligned} P_{\text{FA}} &= {}_2F_1\left(1, \frac{3}{2};\ K+\frac{1}{2}; -\frac{\lambda}{K}\right) \\ &= \frac{2K-1}{2K-z-3}\left\{1 + \frac{2\left(\frac{1}{2}\right)_{K-1}(z-1)^{K-2}}{(K-2)!z^K}\right. \\ &\quad \times \left[-z + (2K-z-3)\sqrt{z}\tanh^{-1}(\sqrt{z})\right. \\ &\quad \left.\left. - \sum_{k=1}^{K-2}\frac{(k-1)!z^k(k-K+z+1)}{\left(\frac{1}{2}\right)_K(z-1)^k}\right]\right\}, \end{aligned} \tag{20}$$

where the last equation is derived with [29].

To facilitate setting the detection threshold in other cases, we provide an approximate expression (in terms of elementary functions) for (14). According to [30, eq. 24],

the probability of false alarm in (14) can be approximated as

$$P_{\mathrm{FA}} \approx \left(K+\frac{1}{2}\right)^{K} r_{2,1}^{-1/2}\left(\frac{y}{M}\right)^{M}\left(\frac{1-y}{K-M+\frac{1}{2}}\right)^{K-M+\frac{1}{2}} \times (1-xy)^{-M-\frac{1}{2}}, \tag{21}$$

where

$$x = -\frac{\lambda}{K}, \tag{22}$$

$$r_{2,1} = \frac{y^2}{M} + \frac{(1-y)^2}{K-M+\frac{1}{2}} - \frac{(M+\frac{1}{2})x^2y^2(1-y)^2}{M(K-M+\frac{1}{2})(1-xy)^2}, \tag{23}$$

$$y = \frac{2M}{\sqrt{\epsilon^2 - 4Mx(K-M)} - \epsilon} \tag{24}$$

with

$$\epsilon = \frac{x}{2} - K - \frac{1}{2}. \tag{25}$$

As shown in Section V, the approximate accuracy of (21) is very high.

Note that the exact expressions in (17) and (20), and the approximate expression in (21) are represented in finite sums of well-known elementary functions, which are easier to use than the hypergeometric function in (14).

B. Probability of Detection

Note that [1] did not provide an expression for the detection probability of the PS-AMF, which is considered in the following. We first derive an exact detection probability for the case of m odd. Next, we discuss how to deal with the case of m even.

As derived in the Appendix, (13) can be equivalently written as

$$\frac{v}{\tau} \underset{H_0}{\overset{H_1}{\gtrless}} \frac{\lambda}{K}\rho, \tag{26}$$

where the distributions of v, τ, and ρ are given by (55), (51), and (52), respectively. Moreover, the random variables v and τ are independent of each other. According to (51), the probability density function (pdf) of τ under H_1 is

$$p(\tau|H_1) = \frac{1}{\Gamma(M)}\tau^{M-1}\exp(-\tau), \quad \tau > 0. \tag{27}$$

Actually, τ under H_1 has a Gamma distribution with shape M and scale 1. From (55), the pdf of v under H_1 is

$$p(v|H_1) = \exp[-(v+\xi)]I_0(2\sqrt{\xi v}), \quad v > 0, \tag{28}$$

where I_r is the modified Bessel function of the first kind.

1) *Nonfluctuating Target Model*: Here, we examine the nonfluctuating target model where a is deterministic. Define

$$\omega = \frac{\lambda\rho}{K}\tau. \tag{29}$$

Based on (27), the pdf of ω conditioned on ρ can be expressed as

$$p(\omega|\rho) = \frac{K}{\lambda\rho\Gamma(M)}\left(\frac{K}{\lambda\rho}\right)^{M-1}\omega^{M-1}\exp\left(-\frac{K\omega}{\lambda\rho}\right). \tag{30}$$

Therefore, the detection probability of the PS-AMF conditioned on ρ is

$$\begin{aligned} P_{\mathrm{D}|\rho} &= \int_0^{+\infty}\left(\int_{\omega}^{+\infty} p(v|\,H_1)\mathrm{d}v\right)p(\omega|\rho)\,\mathrm{d}\omega \\ &= 1 - \left(1+\frac{\lambda\rho}{K}\right)^{-M}\sum_{j=1}^{M}\mathrm{C}_M^j\left(\frac{\lambda\rho}{K}\right)^j \\ &\quad\times \exp\left(-\frac{\rho\zeta}{1+\frac{\lambda\rho}{K}}\right)\sum_{n=0}^{j-1}\frac{1}{n!}\left(\frac{\rho\zeta}{1+\frac{\lambda\rho}{K}}\right)^n, \end{aligned} \tag{31}$$

where the second equality is obtained by using [31, eq. (4-16)]. Furthermore, the unconditional probability of detection for m odd is obtained by averaging over ρ, i.e.,

$$P_{\mathrm{D}} = \int_0^1 P_{\mathrm{D}|\rho}p(\rho)\mathrm{d}\rho, \tag{32}$$

where $p(\rho)$ is the distribution of ρ given by [see (52)]

$$p(\rho) = \left[B\left(M+\frac{1}{2},\frac{m-1}{2}\right)\right]^{-1}\rho^{M-\frac{1}{2}}(1-\rho)^{\frac{m-3}{2}}, \tag{33}$$

where $B(\cdot,\cdot)$ denotes the Beta function.

Note that the above derivation of the detection probability in (32) is based on the assumption of m odd. When m is even, unfortunately, a closed-form expression for the probability of false alarm is intractable. Intuitively, we can approximate the detection probability for m even as the arithmetic mean of the detection probabilities obtained by replacing m with m –1 and $m+1$ in (32). Number simulations in Section IV show that the approximate results match the MC simulation results pretty well.

2) *Fluctuating Target Model*: In the above analysis we assumed that the amplitude a of the target is deterministic. In many practical scenarios, a may be described better with a fluctuating model where a is random [27, 32]. Therefore, it is of interest to examine how the detector performs with a fluctuating target model. It should be pointed out that the PS-AMF is developed for the nonfluctuating target model, not for the fluctuating one. Therefore, there exists a mismatched signal model when the PS-AMF is applied to the fluctuating target model. Nevertheless, similar examinations of detectors derived for nonfluctuating targets in fluctuating cases are considered in many studies (e.g., [3, 11]).

Let $a = |a|\exp(\jmath\theta)$. The phase θ is often assumed to be uniformly distributed within the interval $[0, 2\pi)$, while many pdfs have been used to describe the statistical characterization of the amplitude $|a|$. We consider that $|a|$ has a generalized Chi distribution [27, 32–34], namely, the

pdf of $|a|$ is

$$p_{|a|}(r) = \frac{2L^L r^{2L-1}}{\sigma_a^{2m}\Gamma(L)} \exp\left(-\frac{Lr^2}{\sigma_a^2}\right), \quad r > 0, \tag{34}$$

where L and σ_a^2 are the shape and scale parameters, respectively. Note that the above distribution in (34) includes the Rayleigh distribution as a special case with $L = 1$. In this special case, a is a complex Gaussian variable, i.e., $a \sim \mathcal{CN}(0, \sigma_a^2)$.

Define

$$\delta = \sigma_a^2 \mathbf{s}^T \mathbf{R}^{-1} \mathbf{s}, \tag{35}$$

and

$$\phi = \sigma_a^{-2}|a|^2. \tag{36}$$

Then, ζ defined in (57) can be rewritten as $\zeta = \delta\,\phi$. Based on (34), we can derive the pdf of ϕ as

$$p_\phi(\phi) = \frac{L^L \phi^{L-1}}{\Gamma(L)} \exp(-L\phi), \quad \phi > 0. \tag{37}$$

Therefore, the detection probability of the PS-AMF with m odd, conditioned on ρ for the fluctuating target model, can be expressed as

$$\begin{aligned}\tilde{P}_{\mathrm{D}|\rho} &= \int_0^{+\infty} P_{\mathrm{D}|\rho}\, p_\phi(\phi)\mathrm{d}\phi \\ &= 1 - \left(1 + \frac{\lambda\rho}{K}\right)^{-M} \sum_{j=1}^{M} \mathrm{C}_M^j \left(\frac{\lambda\rho}{K}\right)^j \sum_{n=0}^{j-1} \frac{L^L \Gamma(n+L)}{n!\Gamma(L)} \\ &\quad \times \left(\frac{\rho\delta}{1+\frac{\lambda\rho}{K}}\right)^n \left(L + \frac{\rho\delta}{1+\frac{\lambda\rho}{K}}\right)^{-(n+L)}.\end{aligned} \tag{38}$$

Furthermore, the unconditional detection probability of the PS-AMF with m odd for the fluctuating target model is

$$\tilde{P}_{\mathrm{D}} = \int_0^1 \tilde{P}_{\mathrm{D}|\rho}\, p(\rho)\mathrm{d}\rho, \tag{39}$$

where $p(\rho)$ is defined in (33).

We now turn to the case where m is even. In such a case, we can obtain an approximate detection probability of the PS-AMF for the fluctuating model, in an intuitive way similar to that in the case of nonfluctuating target model. More precisely, the detection probability with m even in the fluctuating target model can be approximated as the arithmetic mean of the detection probabilities obtained by replacing m with $m-1$ and $m+1$ in (39).

IV. SIMULATION RESULTS

In this section, numerical simulations are conducted to confirm the validity of the above theoretical results. Without loss of generality, we select $\mathbf{s} = [1, 1, \ldots, 1]^T$. The (i, j)th element of the noise covariance matrix is chosen to be $[\mathbf{R}]_{i,j} = \sigma^2 \tilde{\rho}^{|i-j|}$, where $\tilde{\rho}$ is the correlation coefficient, and σ^2 represents the noise power and is set to be 1. It should be pointed out that many values of $\tilde{\rho}$, such as 0.9 and 0.99, have been used in simulations. It is shown that the PS-AMF works well with these values. Here, we choose the simulation results with $\tilde{\rho} = 0.9$ for illustration.

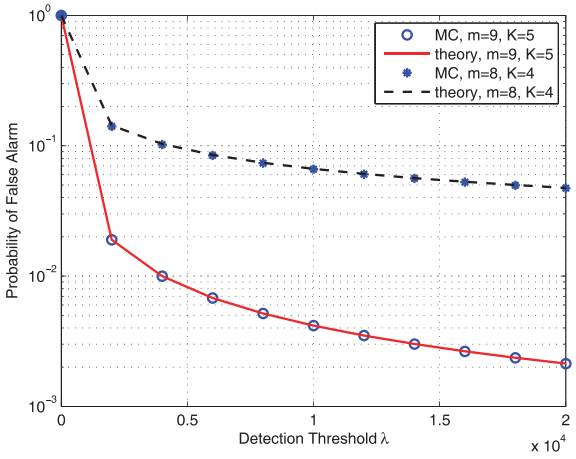

Fig. 1. Probability of false alarm calculated with exact but elementary expressions in (17) and (20).

For comparison purposes, we introduce the MF detector and the AMF. The MF detector can be written as

$$\Lambda_{\mathrm{MF}} = \frac{|\mathbf{p}^\dagger \mathbf{M}^{-1}\mathbf{x}|^2}{\mathbf{p}^\dagger \mathbf{M}^{-1}\mathbf{p}} \underset{H_0}{\overset{H_1}{\gtrless}} \lambda_{\mathrm{MF}}, \tag{40}$$

where λ_{MF} is the detection threshold. Note that the MF detector cannot be implemented in practice, since it assumes that the noise covariance matrix is known. However, it can provide a benchmark against which we can compare the detection performance of the proposed detectors. The AMF is [3]

$$\Lambda_{\mathrm{AMF}} = \frac{|\mathbf{p}^\dagger \hat{\mathbf{M}}^{-1}\mathbf{x}|^2}{\mathbf{p}^\dagger \hat{\mathbf{M}}^{-1}\mathbf{p}} \underset{H_0}{\overset{H_1}{\gtrless}} \lambda_{\mathrm{AMF}}, \tag{41}$$

where $\hat{\mathbf{M}} = \frac{1}{K}\sum_{k=1}^{K} \mathbf{y}_k \mathbf{y}_k^\dagger$ and λ_{AMF} is the detection threshold.

In Fig. 1, the probability of false alarm as a function of the detection threshold is depicted for $m = 8$ and $m = 9$. The number of secondary data is selected to be the minimum value required, i.e., $K = 4$ for $m = 8$ in case 1 and $K = 5$ for $m = 9$ in case 2. Note that the dashed and solid lines denote the results obtained by using the exact but elementary expressions in (17) and (20), respectively. The symbols "○" and "*" denote the results obtained with MC simulations. The number of independent trials used in each case is 100 000. It is shown that the analytical results are in good agreement with the simulation results.

In Fig. 2, we examine the general case. The lines denote the approximate thresholds obtained using (21) instead of (14), and the symbols denote the results obtained by MC simulations. It can be seen from Fig. 2 that the approximate results match the simulation results pretty well. It means that the integral in (14) can be approximated well by the elementary expression in (21).

Performance comparisons between the MF, AMF, and PS-AMF detectors in the deterministic target model are presented for $m = 8$ and $m = 9$ in Figs. 3 and 4,

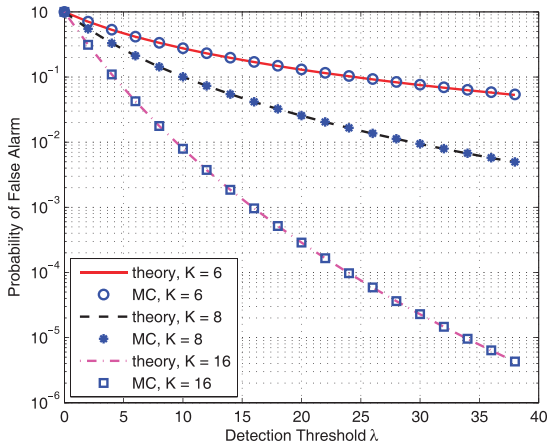

Fig. 2. Probability of false alarm calculated with approximate but elementary expression in (21) for $m = 8$.

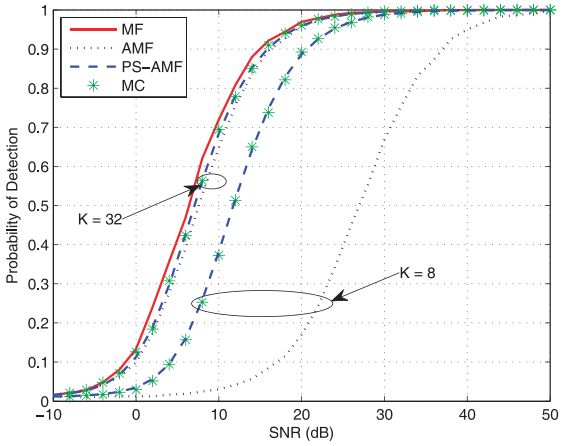

Fig. 5. Performance comparisons in fluctuating target model for even $m = 8$.

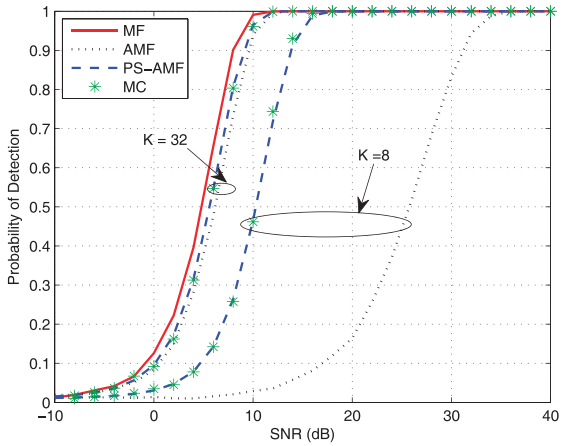

Fig. 3. Performance comparisons in nonfluctuating target model for even $m = 8$.

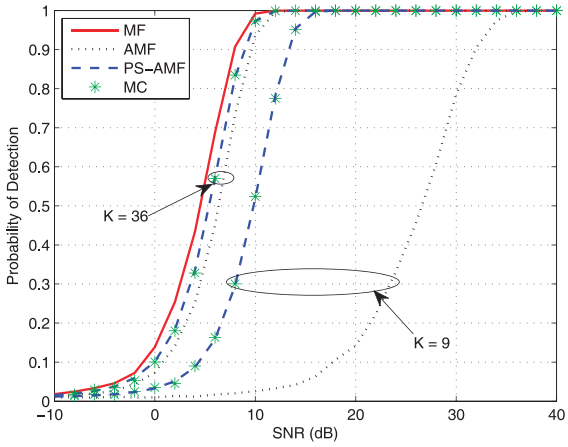

Fig. 4. Performance comparisons in nonfluctuating target model for odd $m = 9$.

respectively. The detection probability curves of the PS-AMF (i.e., the dashed lines) in Figs. 3 and 4 are depicted by using the intuitive approximation method and (32), respectively. The detection probability curves of the MF detector and the AMF (i.e., the solid and dotted lines, respectively), and the symbol * are plotted by using MC simulations. The number of independent trials used to calculate the detection probability in each case is 5 000, and the detection threshold is obtained by using the theoretical expression. Obviously, the theoretical results are in good accordance with the simulation results.

It is demonstrated that the PS-AMF significantly outperforms the AMF, especially when the number of secondary data is small (for instance, $K = 8$ in Fig. 3 and $K = 9$ in Fig. 4). This is due to the fact that the PS-AMF exploits a priori knowledge about the persymmetric structure of the noise covariance matrix. In addition, we can see that the detection performance of the AMF and PS-AMF improves as the number of secondary data increases. Interestingly, the AMF and PS-AMF detectors perform almost the same as the MF detector when the number of secondary data is sufficiently large (for example, $K = 32$ in Fig. 3 and $K = 36$ in Fig. 4). This is expected, since one can obtain high accuracy in the noise covariance matrix estimate by using sufficient secondary data, even without a priori information on the persymmetric structure.

In Figs. 5 and 6 we make performance comparisons in the random model. All the parameters except L in Figs. 5 and 6 are the same as those in Figs. 3 and 4, respectively. Here, we select $L = 1$, which means that the complex amplitude a has a complex Gaussian distribution. Note that the detection probability curves of the PS-AMF (i.e., the dashed lines) in Figs. 5 and 6 are plotted by the intuitive approximation method and (39), respectively. The solid and dashed lines, and the symbol * are all depicted by the MC simulations. It can be seen that in the stochastic model the analytical results also agree with the simulation results. In addition, the relationship among the detection performance of the three detectors in Figs. 5 and 6 is the same as in Figs. 3 and 4, respectively. We can use the same reasons to explain the phenomenon.

The impact of the scale parameter L on the detection performance of the PS-AMF is presented in Fig. 7, where $m = 9$ and $K = 12$. These detection probability curves are

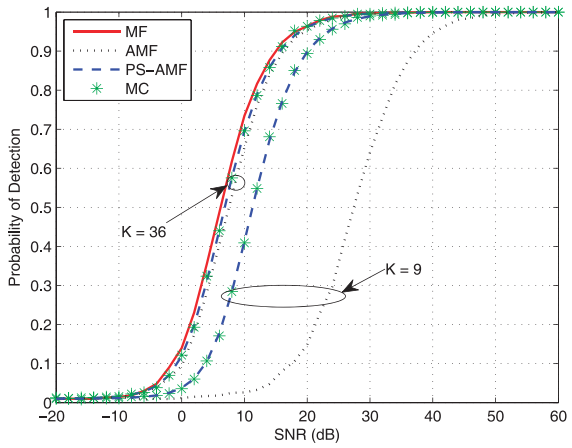

Fig. 6. Performance comparisons in fluctuating target model for odd $m = 9$.

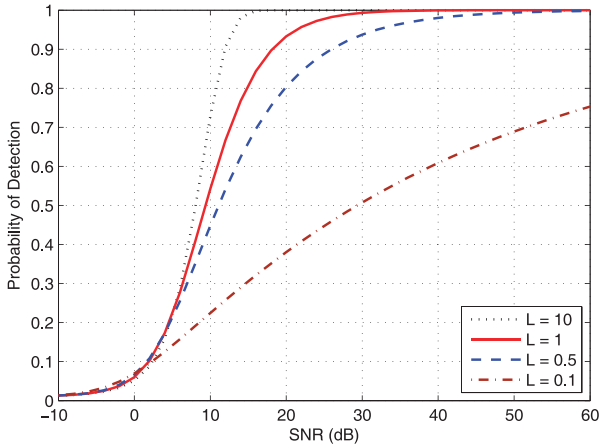

Fig. 7. Detection performance for different L with $m = 9$ and $K = 12$.

obtained by using (39). One can observe that as L decreases, the detection performance improves in the low signal-to-noise ratio (SNR) region (e.g., SNR $\in$ [–10, 0] dB in this example), but decreases in the high SNR region. This phenomenon can be easily explained. In fact, the depth of the amplitude fluctuation is ruled by the scale parameter L. More precisely, the lower the scale parameter L, the wider the fluctuation span. Wide fluctuation spans can result in a gain in the detection performance for a low SNR, but lead to a loss in the detection performance for a high SNR.

V. CONCLUSION

The problem of detecting a target embedded in colored noise with an unknown covariance matrix is considered by exploiting the persymmetric structures in the received signal. This problem can be handled with the PS-AMF proposed in [1]. Two elementary expressions for the probability of false alarm of the PS-AMF are obtained in two training-limited cases where the number of secondary data is only about half of the dimension of the received data. In other cases, we derive an approximate but elementary expression for the probability of false alarm, based on the Laplace approximation to the Gaussian hypergeometric function. It is easier to set the detection threshold by employing these derived elementary expressions than the original hypergeometric function. More importantly, the detection probabilities of the PS-AMF for both nonfluctuating and fluctuating target models are obtained in terms of one-dimensional integral forms. Numerical simulations demonstrate that these theoretical results match the MC simulation results very well. Our analytical results can serve as a set of mathematical tools for the design and evaluation of the PS-AMF.

It should be pointed out that in the current study we do not consider the mismatched case where the actual noise covariance matrix deviates from being persymmetric. Development of robust detection algorithms to deal with such mismatch is a future work.

APPENDIX. EQUIVALENT TRANSFORMATION OF $\Lambda_{\text{PS-AMF}}$

Define $\mathbf{e}_1 = [1, 0, \ldots, 0]^T \in \mathbb{R}^m$. There always exists a real orthogonal matrix $\mathbf{U}$ such that

$$\mathbf{e}_1 = \frac{\mathbf{U}\mathbf{R}^{-1/2}\mathbf{s}}{(\mathbf{s}^\dagger\mathbf{R}^{-1}\mathbf{s})^{1/2}}. \tag{42}$$

Let

$$\mathbf{z} = \mathbf{U}\mathbf{R}^{-1/2}\mathbf{x}, \tag{43}$$

and

$$\hat{\mathbf{W}} = \mathbf{U}\mathbf{R}^{-1/2}(2K\hat{\mathbf{R}})\mathbf{R}^{-T/2}\mathbf{U}^T. \tag{44}$$

It is easy to check that

$$\mathbf{z} \sim \begin{cases} \mathcal{CN}(\mathbf{0}, \mathbf{I}), & \text{under } H_0 \\ \mathcal{CN}(a\mathbf{U}\mathbf{R}^{-1/2}\mathbf{s}, \mathbf{I}), & \text{under } H_1 \end{cases} \tag{45}$$

and

$$\hat{\mathbf{W}} \sim \mathcal{W}_m(2K, \mathbf{I}). \tag{46}$$

Moreover, the test statistic $\Lambda_{\text{PS–AMF}}$ in (13) can be rewritten as

$$\begin{aligned} \Lambda_{\text{PS–AMF}} &= 2K\frac{|\mathbf{e}_1^T\hat{\mathbf{W}}^{-1}\mathbf{z}|^2}{\mathbf{e}_1^T\hat{\mathbf{W}}^{-1}\mathbf{e}_1} \\ &\triangleq \frac{Kv}{\tau\rho}, \end{aligned} \tag{47}$$

where

$$v = \frac{|\mathbf{e}_1^T\hat{\mathbf{W}}^{-1}\mathbf{z}|^2}{\mathbf{e}_1^T\hat{\mathbf{W}}^{-2}\mathbf{e}_1}, \tag{48}$$

$$\tau = \frac{1}{2\mathbf{e}_1^T\hat{\mathbf{W}}^{-1}\mathbf{e}_1}, \tag{49}$$

and

$$\rho = \frac{(\mathbf{e}_1^T\hat{\mathbf{W}}^{-1}\mathbf{e}_1)^2}{\mathbf{e}_1^T\hat{\mathbf{W}}^{-2}\mathbf{e}_1}. \tag{50}$$

Following a line of reasoning similar to that in [1, Appendix A], the distribution of τ is

$$\tau \sim \frac{1}{2}\chi^2_{2K-m+1}, \tag{51}$$

and the distribution of ρ is

$$\rho \sim \beta\left(\frac{2K-m+2}{2}, \frac{m-1}{2}\right). \tag{52}$$

Moreover, τ and ρ are independent of each other.

In the following, our focus is to analyze the statistical properties of the random variable v under hypothesis H_0 and hypothesis H_1. To this end, we introduce a unit-norm vector

$$\mathbf{v} = \frac{\hat{\mathbf{W}}^{-1}\mathbf{e}_1}{\left(\mathbf{e}_1^T\hat{\mathbf{W}}^{-2}\mathbf{e}_1\right)^{-1/2}}. \tag{53}$$

Then, v can be rewritten as

$$v = \mathbf{z}^\dagger\mathbf{P}_\mathbf{v}\mathbf{z}, \tag{54}$$

where $\mathbf{P}_\mathbf{v} = \mathbf{v}\mathbf{v}^\dagger$ is the projection matrix onto the subspace spanned by the vector $\mathbf{v}$. Due to (45), we can obtain that the distribution of v conditioned on ρ is

$$v \sim \begin{cases} \frac{1}{2}\chi^2_2, & \text{under } H_0, \\ \frac{1}{2}\chi'^2_2(2\xi), & \text{under } H_1, \end{cases} \tag{55}$$

where

$$\begin{aligned} \xi &= |a|^2\mathbf{s}^T\mathbf{R}^{-1/2}\mathbf{U}^T\mathbf{P}_\mathbf{v}\mathbf{U}\mathbf{R}^{-1/2}\mathbf{s} \\ &= \frac{|a|^2\mathbf{s}^T\mathbf{R}^{-1/2}\mathbf{U}^T\hat{\mathbf{W}}^{-1}\mathbf{e}_1\mathbf{e}_1^T\hat{\mathbf{W}}^{-1}\mathbf{U}\mathbf{R}^{-1/2}\mathbf{s}}{\mathbf{e}_1^T\hat{\mathbf{W}}^{-2}\mathbf{e}_1} \\ &= |a|^2\mathbf{s}^T\mathbf{R}^{-1}\mathbf{s}\frac{\left(\mathbf{e}_1^T\hat{\mathbf{W}}^{-1}\mathbf{e}_1\right)^2}{\mathbf{e}_1^T\hat{\mathbf{W}}^{-2}\mathbf{e}_1} \\ &= \zeta\,\rho, \end{aligned} \tag{56}$$

where the third equality is obtained by (42), ρ is defined in (50) and

$$\zeta = |a|^2\mathbf{s}^T\mathbf{R}^{-1}\mathbf{s}. \tag{57}$$

Applying (47) to (13) results in (26).

REFERENCES

[1] Pailloux, G., Forster, P., Ovarlez, J.-P., and Pascal, F.
Persymmetric adaptive radar detectors.
IEEE Transactions on Aerospace and Electronic Systems, **47**, 4 (Oct. 2011), 2376–2390.

[2] Kelly, E. J.
An adaptive detection algorithm.
IEEE Transactions on Aerospace and Electronic Systems, **AES-22**, 1 (Mar. 1986), 115–127.

[3] Robey, F. C., Fuhrmann, D. R., Kelly, E. J., and Nitzberg, R.
A CFAR adaptive matched filter detector.
IEEE Transactions on Aerospace and Electronic Systems, **28**, 1 (Jan. 1992), 208–216.

[4] Kraut, S., Scharf, L. L., and McWhorter, L. T.
Adaptive subspace detectors.
IEEE Transactions on Signal Processing, **49**, 1 (Jan. 2001), 1–16.

[5] Kraut, S., Scharf, L. L., and Butler, R. W.
The adaptive coherence estimator: A uniformly-most-powerful-invariant adaptive detection statistic.
IEEE Transactions on Signal Processing, **53**, 2 (Feb. 2005), 417–438.

[6] Jin, Y., and Friedlander, B.
A CFAR adaptive subspace detector for second-order Gaussian signals.
IEEE Transactions on Signal Processing, **53**, 3 (Mar. 2005), 871–884.

[7] Liu, J., Zhang, Z.-J., Shui, P.-L., and Liu, H.
Exact performance analysis of an adaptive subspace detector.
IEEE Transactions on Signal Processing, **60**, 9 (Sept. 2012), 4945–4950.

[8] He, Q., Lehmann, N. H., Blum, R. S., and Haimovich, A. M.
MIMO radar moving target detection in homogeneous clutter.
IEEE Transactions on Aerospace and Electronic Systems, **46**, 3 (July 2010), 1290–1301.

[9] Chong, C. Y.
Signal processing for MIMO radars: Detection under Gaussian and non-Gaussian environments and application to STAP.
Ph.D. thesis, Supelec, France, Nov. 2011.

[10] Liu, J., Zhang, Z.-J., Cao, Y., and Yang, S.
A closed-form expression for false alarm rate of adaptive MIMO-GLRT detector with distributed MIMO radar.
Signal Processing, **93**, 9 (Sept. 2013), 2771–2776.

[11] De Maio, A., and Ricci, G.
A polarimetric adaptive matched filter.
Signal Processing, **81**, 12 (Dec. 2001), 2583–2589.

[12] Pastina, D., Lombardo, P., and Bucciarelli, T.
Adaptive polarimetric target detection with coherent radar Part I: Detection against Gaussian background.
IEEE Transactions on Aerospace and Electronic Systems, **37**, 4 (Oct. 2001), 1194–1206.

[13] Reed, I. S., Mallett, J. D., and Brennan, L. E.
Rapid convergence rate in adaptive arrays.
IEEE Transactions on Aerospace and Electronic Systems, **AES-10**, 6 (1974), 853–863.

[14] Monga, V., and Rangaswamy, M.
Rank constrained ML estimation of structured covariance matrices with applications in radar target detection.
In *IEEE 2012 Radar Conference (RADAR)*, pp. 0475–0480.

[15] Cai, L., and Wang, H.
A persymmetric multiband GLR algorithm.
IEEE Transactions on Aerospace and Electronic Systems, **28**, 3 (July 1992), 806–816.

[16] Ye, Z., and Xu, X.
DOA estimation by exploiting the symmetric configuration of uniform linear array.
IEEE Transactions on Antennas and Propagation, **55**, 12 (Dec. 2007), 3716–3720.

[17] Casillo, M., De Maio, A., Iommelli, S., and Landi, L.
A persymmetric GLRT for adaptive detection in partially-homogeneous environment.
IEEE Signal Processing Letters, **14**, 12 (Dec. 2007), 1016–1019.

[18] Zhang, L., Liu, W., and Yu, L.
Performance analysis for finite sample MVDR beamformer with forward backward processing.
IEEE Transactions on Signal Processing, **59**, 5 (May 2011), 2427–2431.

[19] Nitzberg, R.
Application of maximum likelihood estimation of persymmetric covariance matrices to adaptive processing.
IEEE Transactions on Aerospace and Electronic Systems, **AES-16**, 1 (Jan. 1980), 124–127.

[20] Cai, L., and Wang, H.

A persymmetric modified-SMI algorithm.
Signal Processing, **23**, 1 (Jan. 1991), 27–34.

[21] Conte, E., and De Maio, A.
Exploiting persymmetry for CFAR detection in compound-Gaussian clutter.
IEEE Transactions on Aerospace and Electronic Systems, **39**, 2 (Apr. 2003), 719–724.

[22] Hao, C., Orlando, D., Ma, X., and Hou, C.
Persymmetric Rao and Wald tests for partially homogeneous environment.
IEEE Signal Processing Letters, **19**, 9 (Sept. 2012), 587–590.

[23] Wang, P., Sahinoglu, Z., Pun, M.-O., and Li, H.
Persymmetric parametric adaptive matched filter for multichannel adaptive signal detection.
IEEE Transactions on Signal Processing, **60**, 6 (June 2012), 3322–3328.

[24] Hao, C., Orlando, D., Foglia, G., Ma, X., Yan, S., and Hou, C.
Persymmetric adaptive detection of distributed targets in partially-homogeneous environment.
Digital Signal Processing, **24** (Jan. 2014), 42–51.

[25] De Maio, A., and Orlando, D.
An invariant approach to adaptive radar detection under covariance persymmetry.
IEEE Transactions on Signal Processing, **63**, 5 (Mar. 2015), 1297–1309.

[26] Liu, J., Zhang, Z.-J.,Yang, Y., and Liu, H.
A CFAR adaptive subspace detector for first-order or second-order Gaussian signals based on a single observation.
IEEE Transactions on Signal Processing, **59**, 11 (Nov. 2011), 5126–5140.

[27] De Maio, A.
Robust adaptive radar detection in the presence of steering vector mismatches.
IEEE Transactions on Aerospace and Electronic Systems, **41**, 4 (Oct. 2005), 1322–1337.

[28] Prudnikov, A. P., Brychkov, Y. A., and Marichev, O. I.
Integrals and Series, Vol. **3**. Amsterdam: Gorden and Breach Science Publishers, 1986.

[29] The Wolfram function site. [Online]. Available: http://functions.wolfram.com/07.23.03.0687.01

[30] Butler, R. W., and Wood, A. T. A.
Laplace approximations for hypergeometric functions with matrix argument.
The Annals of Statistics, **30**, 4 (Aug. 2002), 1155–1177.

[31] Kelly, E. J.
Finite-sum expression for signal detection probabilities.
Lincoln Laboratory, MIT, Technical Report 566, 1981.

[32] De Maio, A., Farina, A., and Foglia, G.
Target fluctuation models and their application to radar performance prediction.
IEE Proceedings - Radar, Sonar and Navigation, **151**, 5 (Oct. 2004), 261–269.

[33] Cui, G., De Maio, A., and Piezzo, M.
Performance prediction of the incoherent radar detector for correlated generalized Swerling-Chi fluctuating targets.
IEEE Transactions on Aerospace and Electronic Systems, **49**, 1 (Jan. 2013), 356–368.

[34] Cui, G., De Maio, A., Aubry, A., Farina, A., and Kong, L.
Advanced SLB architectures with invariant receivers.
IEEE Transactions on Aerospace and Electronic Systems, **49**, 2 (Apr. 2013), 798–818.

Jun Liu (S'11—M'13) received the B.S. degree in mathematics from Wuhan University of Technology, China, in 2006, the M.S. degree in mathematics from Chinese Academy of Sciences, China, in 2009, and the Ph.D. degree in electrical engineering from Xidian University, China, in 2012.

From July 2012 to December 2012, he was a Post-doctoral Research Associate in the Department of Electrical and Computer Engineering, Duke University, Durham, NC. From January 2013 to September 2014, he was a Post-doctoral Research Associate in the Department of Electrical and Computer Engineering, Stevens Institute of Technology, Hoboken, NJ. He is now with the National Laboratory of Radar Signal Processing, Xidian University, where he is an Associate Professor. His research interests include statistical signal processing, optimization algorithms, passive sensing, cognitive radar, and multistatic radar.

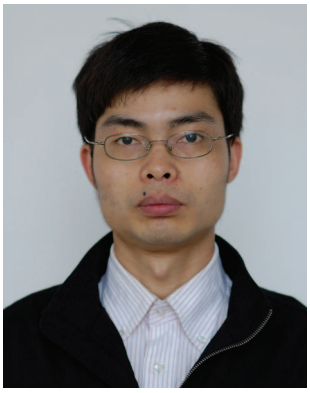

Guolong Cui (M'13) received the B.S., M.S., and Ph.D. degrees from University of Electronic Science and Technology of China, Chengdu, in 2005, 2008, and 2012, respectively.

From January 2011 to April 2011, he was a visiting researcher with University of Naples Federico II, Naples, Italy. From June 2012 to August 2013, he was a postdoctoral researcher in the Department of Electrical and Computer Engineering, Stevens Institute of Technology, Hoboken, NJ. Since September 2013, he has been an Associate Professor in University of Electronic Science and Technology of China, Chengdu. His current research interests include adaptive signal processing and statistical signal processing with emphasis on radars, and waveform optimization.

Hongbin Li (M'99—SM'08) received the B.S. and M.S. degrees from the University of Electronic Science and Technology of China, in 1991 and 1994, respectively, and the Ph.D. degree from the University of Florida, Gainesville, in 1999, all in electrical engineering.

From July 1996 to May 1999, he was a Research Assistant in the Department of Electrical and Computer Engineering at the University of Florida. Since July 1999, he has been with the Department of Electrical and Computer Engineering, Stevens Institute of Technology, Hoboken, NJ, where he became a Professor in 2010. He was a Summer Visiting Faculty Member at the Air Force Research Laboratory in the summers of 2003, 2004, and 2009. His general research interests include statistical signal processing, wireless communications, and radars.

Dr. Li received the IEEE Jack Neubauer Memorial Award in 2013 from the IEEE Vehicular Technology Soceity, the Outstanding Paper Award from the IEEE AFICON Conference in 2011, the Harvey N. Davis Teaching Award in 2003 and the Jess H. Davis Memorial Award for excellence in research in 2001 from Stevens Institute of Technology, and the Sigma Xi Graduate Research Award from the University of Florida in 1999. He has been a member of the IEEE SPS Signal Processing Theory and Methods Technical Committee (TC) and the IEEE SPS Sensor Array and Multichannel TC, an Associate Editor for *Signal Processing* (Elsevier), *IEEE Transactions on Signal Processing*, *IEEE Signal Processing Letters*, and *IEEE Transactions on Wireless Communications*, as well as a Guest Editor for *IEEE Journal of Selected Topics in Signal Processing* and *EURASIP Journal on Applied Signal Processing*. He has been involved in various conference organization activities, including serving as a General Co-Chair for the 7th IEEE Sensor Array and Multichannel Signal Processing (SAM) Workshop, Hoboken, NJ, 2012. Dr. Li is a member of Tau Beta Pi and Phi Kappa Phi.

Braham Himed (M'90—SM'01—F'07) received his Engineer Degree in electrical engineering from Ecole Nationale Polytechnique of Algiers in 1984, and his M.S. and Ph.D. degrees both in electrical engineering, from Syracuse University, Syracuse, NY, in 1987 and 1990, respectively.

He is a Technical Advisor with the Air Force Research Laboratory, Sensors Directorate, RF Technology Branch, in Dayton OH, where he is involved with several aspects of radar developments. His research interests include detection, estimation, multichannel adaptive signal processing, time series analyses, array processing, adaptive processing, waveform diversity, MIMO, passive radar, and over the horizon radar.

Dr. Himed is the recipient of the 2001 IEEE region I award for his work on bistatic radar systems, algorithm development, and phenomenology. He is the Vice-Chair of the AES Radar Systems Panel. He is the recipient of the 2012 IEEE Warren White award for excellence in radar engineering. He is also a Fellow of AFRL (Class of 2013).